(Preprint) AAS 09-224

THE ENDGAME PROBLEM PART A: V-INFINITY LEVERAGING TECHNIQUE AND THE LEVERAGING GRAPH

Stefano Campagnola * and Ryan P. Russell †

ESA and NASA renewed interest on missions to Europa, Ganymede, Enceladus and Titan poses the question on how to best solve the Endgame problem. Endgames typically aim at a cheap insertion maneuver into the science orbit, and can be designed using either Vinfinity Leveraging Maneuvers (VILMs) or the Multi-Body dynamics. Although historically linked to insertion maneuvers, the endgame problem is symmetric and equally applies to departure. In this paper series, we analyze and draw connections between the two apparently separate approaches, providing insight to the dynamics of multi-body gravity assist problem. In this paper we derive new formula for the VILM and build the Leveraging Graph to be used as a reference guide for designing Endgame tours. We prove that the cost of a VILM sequence decreases when using high altitude flybys (as done in the Multi-Body technique). Finally we find a simple quadrature formula to compute the minimum DV transfer between moons using VILMs, which is the main result of the paper. The Leveraging Graphs and associated formulae are derived in canonical units and therefore apply to any celestial system with a smaller body in a circular orbit around a primary. Specifically we demonstrate the new method to provide rapid calculations of the theoretical floor values for delta v requirements for resonant hopping moon tours in the Saturn and Jupiter systems using the VILM model.

INTRODUCTION

In the recent years both NASA and ESA studied a variety of mission options to the Galilean moons at Jupiter and to the Saturn moons including Enceladus and Titan. A very challenging part of the trajectory design of these missions is the Endgame,[1] the last part of the transfer before the insertion maneuver into the science orbit. The Endgame aims at a low ΔV orbit insertion maneuver. The 'Begingame' is the symmetric problem and starts with a low ΔV escape from an initial orbit around a minor body. Both transfers have been studied, designed and implemented on space missions with two distinct approaches.

The first approach uses the $V_\infty-$ Leveraging Maneuver (VILM) technique, where the combined effect of gravity assists and impulsive maneuvers (at the almost opposite apsidal point of the spacecraft orbit) changes the spacecraft relative velocity to the minor body.[2,3] Typically the transfer is first computed in the linked-conics model (i.e. the zero radius sphere of influence, patched-conics model), and then optimized in a real ephemeris model and patched together to the rest of the trajectory. The VILM approach is very intuitive and quickly provides fast solutions. NASA and ESA use the VILM approach for the design of the Endgame trajectories to Europa,[1,4] Ganymede[5] and Titan. The VILM originates and is used frequently with interplanetary trajectories.[2,3] The Messenger mission to Mercury implements a VILM sequence for the endgame at Mercury;[6] the BepiColombo mission to Mercury implements a low-thrust version of the VILM at Earth and at Mercury,[7] followed by a gravitational capture at Mercury.[8] The Cassini spacecraft performed a VILM at Venus before the last Earth gravity assist.[9] The Juno mission, targeted to launch in 2011, implements a VILM at Earth to reach Jupiter.[10]

The second approach uses the Multi-Body Technique,[11,12] where small ΔVs (if any) are applied when the spacecraft is far from the minor body, typically to target high altitude flyby passages which produce the most favorable effects (e.g. behind or in front of the minor body to increase or decrease the spacecraft energy).

*Ph.D. student, University of Southern California, Aerospace and Mechanical Engineering, 854 Downay Way RRB, Los Angeles, CA 90089-1191, stefano.campagnola@missionanalysis.org

†Assistant Professor, Georgia Institute of Technology, Guggenheim School of Aerospace Engineering, 270 Ferst Drive, Atlanta, GA 30332-0150, ryan.russell@gatech.edu.

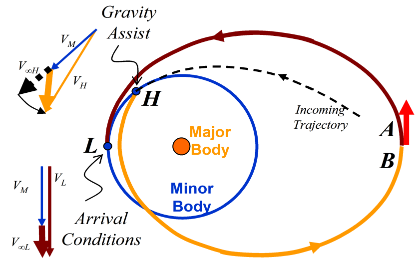

Figure 1 **Example of a $V_\infty-$leveraging maneuver (VILM) to reduce the relative velocity at a minor body: The spacecraft approaches the minor body tangentially and the gravity assist at H rotates the relative velocity $V_{\infty H}$. At the apocenter of the new orbit, the impulsive maneuver changes the shape of the spacecraft orbit so that it becomes tangent again to the minor body orbit at the point H. Although the maneuver actually increases the spacecraft energy, at the point L the spacecraft has a new relative velocity $V_{\infty L} < V_{\infty H}$.**

The trajectory is computed directly in the real ephemeris model, or in the restricted three, four or five body problem. This approach cannot be explained with the linked-conics model, where ballistic transfers cannot change the arrival conditions at the minor body. Trajectories are typically found with some heuristic method. Recently, nonlinear dynamical system theory has been used to help the design of Endgames or MultiMoon orbiters.[4,13] Usually the Multi-body Technique results in low cost, long time of flight trajectories. The Smart1 mission successfully implemented this strategy to get the spacecraft gravitationally captured around the Moon.[12]

In the two papers The Endgame Problem Part A and Part B[14] we study the Endgame transfers in general, and show the connections between the two approaches. The first part of the work, presented in this paper, studies the anatomy of the VILM.

In the first section we derive formulae to show that VILMs are efficient only for V_∞ greater than a minimum value. In the second section we use the formulae to introduce the Leveraging Graph, which has broad endgame design applications. Based on the graph we demonstrate a branch and bound search to globally explore the flight time vs. delta-v solution space. The canonical form of the Leveraging Graphs and formulae are applicable for any planet system or moon system modeled as a smaller body in a circular orbit around a primary. A simple scaling transforms the problem to any dimensioned system of interest. In the third section we define and study the efficiency of the VILM. We prove that the cost of a sequence of VILMs decreases when using high altitude gravity assists (as done when using the Multi-Body Technique). Finally we find the theoretical minimum ΔV for transfer between moons computed using the VILM approach. This new design capability is the main result of the paper.

In the second part of this work, presented in the paper 'The Endgame Problem PARTB', we will focus on the Multi-body Technique and will explain the connection to the VILM approach.

$V_\infty-$LEVERAGING

A $V_\infty-$leveraging maneuver (VILM) is a technique by which a spacecraft orbiting around a major body $(P)^*$ can change its relative speed to a minor body (M).[2,3] The technique consists of a gravity assist and a small impulsive maneuver (ΔV_{AB}) that occurs at opposite apses in the spacecraft orbit around the major body (See Figure 1) . VILMs are typically modeled in the *linked-conics model* (or zero radius sphere of influence, patched-conics model) where the minor body is considered massless and is on a circular orbit around the major body. The spacecraft trajectory is coplanar and starts and ends at the minor body. The gravity assist is modeled as an instantaneous change in the direction of the relative velocity V_∞ by the deviation angle δ. Figure 2 shows the gravity assist geometry.

*For a description of the nomenclature see the section NOTATION at the end of the paper

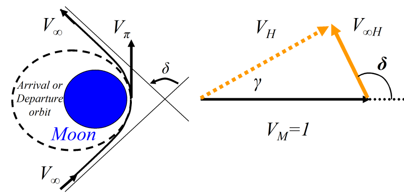

Figure 2 **On the left: The geometry of the gravity assist. The minor body is in the center. On the right: The velocity vectors at the point H which precedes/follows the gravity assist.**

Adimensional variables

Throughout this work we will use adimensional variables, so that the results are general and can be applied to any endgame endgame problem. To obtain the adimensional variables we divide the dimensional variable (denoted with the tilde) by the time and length scale factors:

$$l_{scale} = \tilde{a}_M \qquad t_{scale} = \sqrt{\frac{\tilde{a}_M^3}{\tilde{\mu}_P}}$$

Then the velocity scale factor becomes the velocity of the minor body $\tilde{V}_M$, and the adimensional velocity and the semi-major axis of the minor body and the gravitational constant of the major body are unitary.

We also define V_c as the adimensional velocity of the circular orbit of radius $\tilde{r}_\pi = \tilde{r}_M + \tilde{h}_\pi$ around the minor body:

$$V_c = \sqrt{\frac{\tilde{\mu}_M}{\tilde{r}_\pi}} / \tilde{V}_M$$

This adimensional parameter groups the problem dependency on the minor body gravity constant, minor body radius and altitude of the final/initial orbit insertion/escape.

In adimensional unit the gravity assist deflection angle is: $\delta = 2 \arcsin\left(1/1 + \left(V_\infty/V_c\right)^2\right)$, and the spacecraft velocity at the closest approach to the minor body, V_π, is:

$$V_\pi\left(V_\infty, h_\pi\right) = \sqrt{V_\infty^2 + 2V_c^2} \tag{1}$$

VILM Model and Classification

In this section we refer to Figure 3 to define the general variations and associated relevant variables of the VILM. We assume that the impulsive maneuver is tangential and is performed exactly at the apses. This assumption is typically included when studying VILMs because the Jacobi constant in the rotating frame is maximally changed by performing the maneuver when the rotating velocity is the greatest - this occurs at apses.[15] We also assume that the spacecraft departs/arrives at point L tangent to the minor body. This condition guarantees the lowest $V_{\infty L}$[16] and greatly simplifies the tour problem because we can decouple each VILM as opposed to having to optimize a large sequence of VILMs altogether.

We divide the trajectory into two legs ($A - L$ and $B - H$) joining four different states of the spacecraft (L,A,B,H). At the point L the spacecraft is at an apside with a relative velocity $V_{\infty L}$ w.r.t the minor body. At the point A the spacecraft is at the opposite apsidal point, at a distance r_A from the major body and with a velocity V_A. In between states A and B the spacecraft performs the impulsive maneuver $\Delta V_{AB} = |V_A - V_B|$. At the point H^+ *or* H^- the spacecraft intersects the minor body orbit with a relative velocity $V_{\infty H} > V_{\infty L}$.

We recall from the literature[3] that there are four types of $V_\infty-$leveraging maneuvers, depending on the following features:

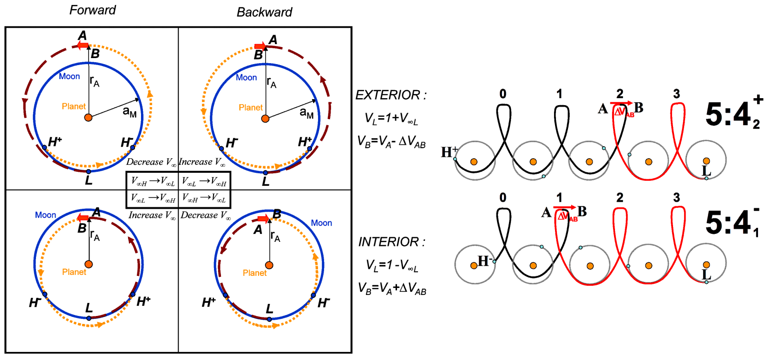

Figure 3 **On the left, four variations of the $V_\infty-$leveraging maneuver (VILM). On the right, schematic of two different $5:4$ VILMs. On the top: the ΔV_{AB} occurs after two full revolutions of the spacecraft on the leg $H^+ - B$. Also, the transfer lasts a bit more than 5 revolutions of the minor body; hence the notation $5:4_2^+$. On the bottom: the ΔV_{AB} occurs after one full revolution of the spacecraft on the leg $H^- - B$. Also, the transfer lasts a bit less than 5 revolutions of the minor body; hence the notation $5:4_1^-$.**

- *Forward (Backward)* if the ΔV_{AB} is in the same (opposite) direction of the spacecraft velocity.
- *Exterior (Interior)* if the ΔV_{AB} occurs at apocenter (pericenter) , thus if $r_A > a_M$ ($r_A < a_M$).

From these definitions it follows that the Forward-Exterior $V_\infty-$leveraging and Backward-Interior $V_\infty-$leveraging *decrease* the V_∞, while the Forward-Interior $V_\infty-$leveraging and Backward-Exterior $V_\infty-$leveraging *increase* the V_∞.

From our definitions it also follows that:

$$V_L^{(E,I)} = 1 \pm V_{\infty L} \tag{2}$$

$$V_A^{(E,I)} = V_B \pm \Delta V_{AB} \tag{3}$$

where the upper sign refers to the Exterior VILM and the lower sign refers to the Interior VILM. Note that from these definitions and from Figure 3 on the left we find boundary values for V_∞. In particular, $0 < V_{\infty L} < \sqrt{2} - 1$ for the Exterior VILM for r_A to be bounded, and $0 < V_{\infty L} < 1$ for the Interior VILM for V_L to be positive.

For each type of VILM we also specify:

- the resonant ratio: $n : m$, where n (m) is the approximate number of the minor body (spacecraft) revolutions during the VILM.
- K number of full revolution in the arc $H - B$ *.
- the point H^-or H^+ where the spacecraft encounters the minor body, resulting in a *long-transfer* VILM or *short-transfer* VILM respectively. Exterior, long-transfer VILMs and Interior, short-transfer VILMs are linked by prograde gravity assists. Exterior, short-transfer VILMs and Interior, long-transfer VILMs are linked by retrograde gravity assists.

As an example, Figure 3 on the right shows the schematic of a $5:4^+$ and of a $5:4^-$VILM. In the rest of the paper we refer to “Backward/Forward, Interior/Exterior $n : m_K^\pm$” VILMs. For example the Europa endgame when approached from Ganymede is a sequence of Forward Exterior VILMs.

*In literature we can find a different choice of letters: $K : L(M)^\pm$ where $K \equiv n$, $L \equiv m$, and $M \equiv K$ for Exterior VILM

Phase-Free Formulae

In this section we present a general formulation which is valid for all the four types of VILM. We start by considering the phase-free problem that does not require the spacecraft and the minor body to be at the points L and $H^{\pm}$ at the same time. The formulae presented in this section are new and allow us to perform many useful, fast, preliminary and global analyses which we present in the next sections. The details of the following calculations are in APPENDIX A.

We first define the function:

$$\Gamma^{(E,I)}\left(V_{\infty L}\right) \equiv \pm\left(r_A - V_A\right) = V_{\infty L}\frac{V_{\infty L}^3 \pm 3V_{\infty L}^2 - V_{\infty L} \mp 7}{V_{\infty L}^3 \pm 3V_{\infty L}^2 + V_{\infty L} \mp 1}$$

where $\Gamma^{(E)}$ is computed for the Exterior VILM , and $\Gamma^{(I)}$ for the interior VILM. If no distinction is necessary we simply refer to Γ. We can show that Γ is a positive strictly monotonic function of V_∞. Later, we will see that Γ is convenient because it provides a minimum bound on V_∞ values where VILMs are useful.

With this notation we can explicitly state the high relative velocity $V_{\infty H}$ as a function of the low relative velocity $V_{\infty L}$ and of the ΔV_{AB}:

$$V_{\infty H}\left(V_{\infty L}, \Delta V_{AB}\right) = \sqrt{\left(V_{\infty L}\right)^2 + \left(\Delta V_{AB}\right)^2 + 2\Delta V_{AB}\Gamma} \tag{4}$$

Equivalently , we can explicitly state the ΔV_{AB} as a function of the high and low relative velocity:

$$\Delta V_{AB}\left(V_{\infty L}, V_{\infty H}\right) = -\Gamma + \sqrt{\Gamma^2 + \left(V_{\infty H}^2 - V_{\infty L}^2\right)} \tag{5}$$

Finally we define the *phase-free efficiency* of the VILM. The phase-free efficiency of Backward-Interior or Forward-Exterior VILM ϵ_{BI-FE} is the increase of the final relative velocity $V_{\infty H}$ due to a change in cost ΔV_{AB}, for a fixed initial relative velocity $V_{\infty L}$:

$$\epsilon_{BI-FE} \equiv \frac{\partial V_{\infty H}}{\partial \Delta V_{AB}} \equiv D_2 V_{\infty H} = \frac{\Delta V_{AB} + \Gamma}{V_{\infty H}\left(V_{\infty L}, \Delta V_{AB}\right)} \tag{6}$$

where D_i is the derivative with respect to the $i-th$ argument. The *phase-free efficiency* of a Backward-Exterior or Forward-Interior VILMs ϵ_{BE-FI} is the decrease of the final relative velocity $V_{\infty L}$ due to a change in cost ΔV_{AB}, for a fixed initial relative velocity $V_{\infty H}$:

$$\epsilon_{BE-FI} \equiv -\frac{\partial V_{\infty L}}{\partial \Delta V_{AB}}$$

We derive an expression for ϵ_{BE-FI} by first taking the partial derivative of $V_{\infty H}$ with respect to $V_{\infty L}$:

$$D_1 V_{\infty H} \equiv \frac{\partial V_{\infty H}}{\partial V_{\infty L}} = \frac{V_{\infty L} + \Delta V_{AB}\frac{d\Gamma}{dV_{\infty L}}}{V_{\infty H}\left(V_{\infty L}, \Delta V_{AB}\right)} \tag{7}$$

We then use the Implicit Function Theorem (see for example[17]) to compute:

$$\epsilon_{BE-FI} = -\frac{\partial V_{\infty L}}{\partial \Delta V_{AB}} = D_2 V_{\infty H} \circ \left[D_1 V_{\infty H}\right]^{-1} = \frac{\Delta V_{AB} + \Gamma}{V_{\infty L} + \Delta V_{AB}\frac{d\Gamma}{dV_{\infty L}}} \tag{8}$$

Phase-Fixed Solutions

In this section we restore the phasing constraint and introduce the concept of Leveraging Graphs. The algorithm to compute the numerical solution to the constrained problem is a variation of the one described for instance in,[3] so we skip the details. In general, given $V_{\infty H}$:

- We assume the minor body and the spacecraft are both at the point H at time t_H;

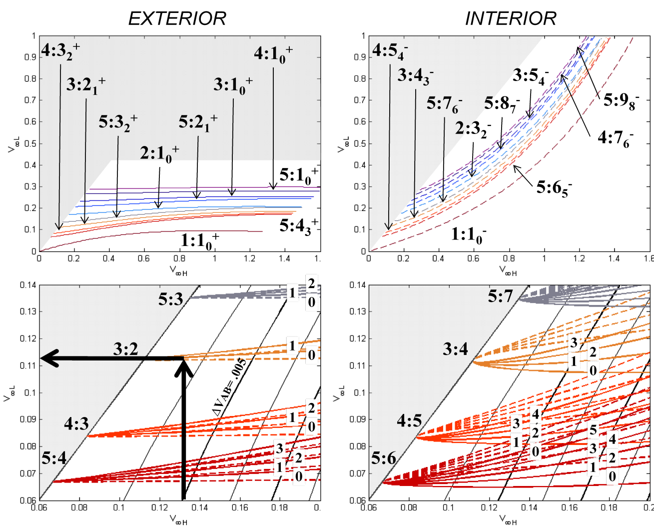

Figure 4 $(V_{\infty L} - V_{\infty H})$ **Leveraging Graph for the Exterior (top left) and Interior (top right) VILM. The domain of feasible** $V_{\infty L}$ **are discussed in the previous section.**

- We guess the flight path angle γ at H (see Figure 2), and find the orbital parameters of the leg $H - B$.
- We compute the orbital parameters of the leg $L - A$ with apses at L and r_A.
- We compute the transfer time and the time t_L when the spacecraft is at L
- We compute the distance from the point L to the position of the minor body at time t_L and differentially correct the path angle γ until the distance vanishes.

The numerical solutions to the VILM problem are one set of $V_{\infty H}\,(V_{\infty L})$ curves for Exterior $m : n_K^{\pm}$ VILMs, and one set of $V_{\infty H}\,(V_{\infty L})$ curves for the Interior $m : n_K^{\pm}$ VILMs. We plot these solutions on a special graph , which we call $(V_{\infty L} - V_{\infty H})$ *Leveraging Graph.* We can also plot these solutions using other variables related to V_∞, thus defining different Leveraging Graphs. In the next section we build and use the *Tisserand Leveraging Graph*. Following this definition, the graphs in literature can be referred as $(r_{aphelion} - V_{\infty Earth})$ *Leveraging Graph* or $(r_{aphelion} - \Delta V_{TOT})$ *Leveraging Graph* etc.([2,3]).

Figure 4 shows the $(V_{\infty L} - V_{\infty H})$ Leveraging Graphs for the Exterior (top left) and Interior (top right) VILM (The domain of feasible $V_{\infty L}$ are discussed in the previous section). In these graphs, for simplicity and clarity, we plot only one VILM (the most efficient) for each $n : m$ case. We emphasize that the leveraging maneuvers and graphs are computed only once in adimensional units, so that they can be applied to any endgame problem using the scale factors. Note that all of the numerical solutions presented in Figure 5 are computed using a 200 line code written in Matlab. The computational time is approximately 1 minute using a dual-core 1.83 GHz laptop processor.

Figure 4 also shows a close-up of the Exterior (bottom left) and Interior (bottom right) VILM. In contrast to the top row, all VILM solutions are plotted for each $n : m$ case. As an example , we show that the $3 : 2$ Exterior VILM reduces the V_∞ from $V_{\infty H} = 0.131$ to $V_{\infty L} = 0.1135$. By plotting the level sets of the phase free function $\Delta V_{AB}(V_{\infty L}, V_{\infty H})$ of Eq. (5) we estimate the $\Delta V_{AB} \approx 0.0022$. For a VILM at Europa, we multiply these values by the average velocity of Europa of approx $13.7km/s$ to find that we decrease $\tilde{V}_{\infty H} = 1.8km/s$ to $\tilde{V}_{\infty L} = 1.56km/s$ using approx. $30m/s$.

Finally we define the *phase-fixed efficiency* E of the VILM as the ratio between the variation of V_∞ and the ΔV_{AB}:

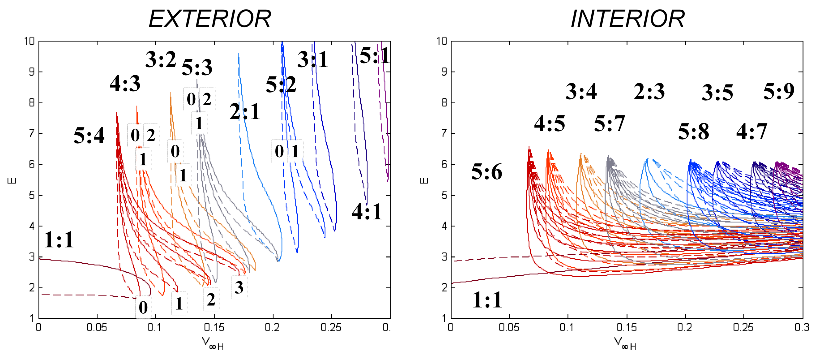

Figure 5. **Efficiency of the Exterior (left) and Interior (right) VILM.**

$$E = \frac{V_{\infty H} - V_{\infty L}}{\Delta V_{AB}}$$

Figure 5 shows the phase-fixed efficiency of the Exterior (left) and Interior (right) VILM. The figure shows the most efficient VILMs are the ones with large K ($K_{best} = m - 1$), and with long or short transfer time for the Exterior or Interior VILM respectively. However, we avoid discarding the less efficient solutions because the difference in efficiency can often be compensated when computing the VILM in more accurate models.

Minimum $V_{\infty L}$

Figure 4 shows that a ΔV_{AB} of approx. $30m/s$ reduces the relative velocity by approx. 240m/s. However it is not always true that the ΔV_{AB} is smaller than the actual gain/loss in relative velocity magnitude at the flyby body. In what follows we show that this occurs only if $V_{\infty L}$ is larger than a given value, which depends on V_c.

Let's assume an endgame problem where the spacecraft initially approaches the minor body with $V_{\infty H}$. The spacecraft needs $\Delta V_{\pi H} = V_{\pi H} - V_c$ to be captured in the target orbit. Alternatively, the spacecraft can perform a VILM which reduces the relative velocity to $V_{\infty L}$, and the new orbit insertion maneuver requires $\Delta V_{\pi L} = V_{\pi L} - V_c$. Then the VILM is efficient as long as the reduction of V_π is greater than the VILM cost ΔV_{AB}.

Proposition The VILM strategy is efficient iff $V_{\infty L} > \overline{V}_\infty$ where $\overline{V}_\infty = \sqrt{\overline{V}_\pi^2 - 2V_c^2}$ and $\overline{V}_\pi\left(V_c\right)$ is the root of the function:

$$f(V_\pi) = \Gamma \circ V_\infty\left(V_\pi; V_c\right) - V_\pi \tag{9}$$

where V_c is a parameter for f, and $\circ$ denotes function composition.

PROOF From Eq. (1) we find:

$$V_{\infty H}^2 = V_{\pi H}^2 - 2V_c^2 \quad , \quad V_{\infty L}^2 = V_{\pi L}^2 - 2V_c^2 \tag{10}$$

We square Eq. (4) and use Eq. (10) to find:

$$\left(V_{\pi H}\right)^2 = \left(V_{\pi L} + \Delta V_{AB}\right)^2 + 2\Delta V_{AB}\left(\Gamma - V_{\pi L}\right)$$

The VILM strategy is efficient if ΔV_{AB} is less than the change in V_π, thus if

$$V_{\pi H} > \left(V_{\pi L} + \Delta V_{AB}\right) \longrightarrow \Gamma - V_{\pi L} > 0$$

To solve the problem we need to study the function $f(V_{\pi L}) = \Gamma \circ V_\infty\left(V_{\pi L}; V_c\right) - V_{\pi L}$, where V_c is a parameter.

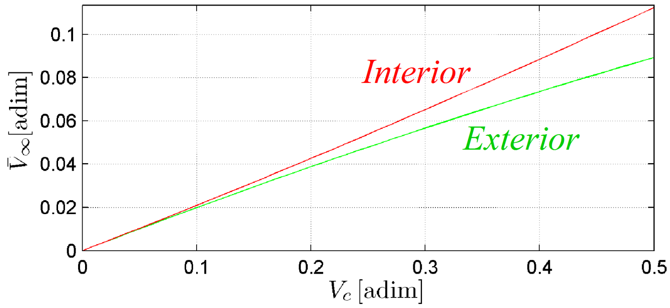

Figure 6. $\overline{V}_\infty$**, minimum value of** V_∞ **for the VILM to be efficient.**

For $V_{\pi L} = \sqrt{2}V_c$, we have $V_{\infty L} = \Gamma = 0$, thus $f(\sqrt{2}V_c) = -V_c$. Also $df/dV_\pi = d\Gamma/dV_{\infty L} * V_{\pi L}/V_{\infty L} - 1 > 0$ *. Then $f(V_\pi) > 0$ iff $V > \overline{V}_\pi$, where $\overline{V}_\pi\,(V_c)$ is the only root of $f\,(V_\pi) = 0$. Note that the root for the Exterior VILM is different from the root of the Interior VILM, as $\Gamma^{(E)} \neq \Gamma^{(I)}$.

Q.E.D.

To compute $\overline{V}_\pi$ we find numerically the root of the function in Eq. (9). Then we use Eq. (1) to find $\overline{V}_\infty$. Figure shows the values of $\overline{V}_\infty$ as function of the parameter V_C. The two curves for the Exterior and Interior case can be approximated by the following cubic splines:

$$\begin{aligned}
\overline{V}^E_\infty &= (5.956166e-5)\,V_c^3 - (5.134491e-2)\,V_c^2 + (2.044185e-1)\,V_c - (7.271228e-6) \\
\overline{V}^I_\infty &= -(1.917650e-2)\,V_c^3 - (5.181414e-2)\,V_c^2 + (2.037734e-1)\,V_c + (8.746307e-6)
\end{aligned}$$

LEVERAGING GRAPH AND THE EUROPA ENDGAME

In this section we introduce the Tisserand Leveraging Graph which we use to design endgame strategies.

The Tisserand graph is a graph representing the Pericenter r_p and Period T of Keplerian coplanar orbit around a major body.[18,19] If one minor body moves on a coplanar circular orbits around the major body, the Tisserand graph shows the *minor body subdomain* , i.e. the set of points (r_p,T) corresponding to the orbits which intersect the minor body orbit. More importantly, the Tisserand graph shows the $V_\infty-$level sets, which are the orbits intersecting the minor body orbit with a constant V_∞. When a spacecraft performs a gravity assist at the minor body, it changes its location on the graph while staying on the $V_\infty-$level set. For this reason the Tisserand graph is a useful graph of the planetary / moon systems, and it has been used to design complicated multiple gravity assist trajectories.[20,21,16]

The Tisserand Leveraging Graph is an extension of the Tisserand graph which includes the numerical solutions of the VILM. Because we use adimensional units we only need to compute the graph once, and then scale it for the different minor bodies we want to include. To build the graph we begin by computing the Tisserand graph (See[18,19]) and representing it with the apocenter on the $x-$axis and the pericenter on the $y-$axis. This choice of the axes results in rectangular, semi-infinite sub domains of the minor bodies, and in period level sets which are straight diagonal lines with a slope of -1. Starting with a (r_a, r_p) orbit, the new (r_a, r_p) following a VILM is aligned horizontally or vertically with the initial state. In particular:

- The ΔV_{AB} of the Interior VILM changes the apocenter but not the pericenter of the initial orbit. We represent the Interior VILM with a horizontal shift from/to the left boundary of the minor body subdomain.

*An expression for $d\Gamma/dV_{\infty L}$ is given in APPENDIX A

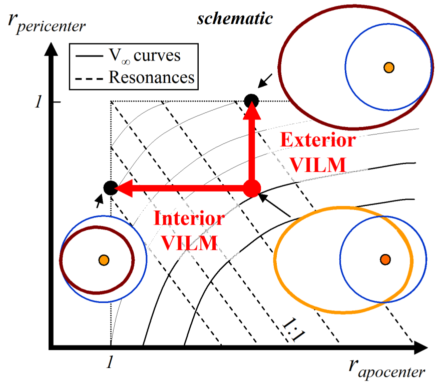

Figure 7 **A schematic apocenter-pericenter Tisserand graph and the effect of an Interior and Exterior VILM. We also plot the period level sets and the V_∞ level sets. We clearly see how the ΔV_{AB} changes the V_∞.**

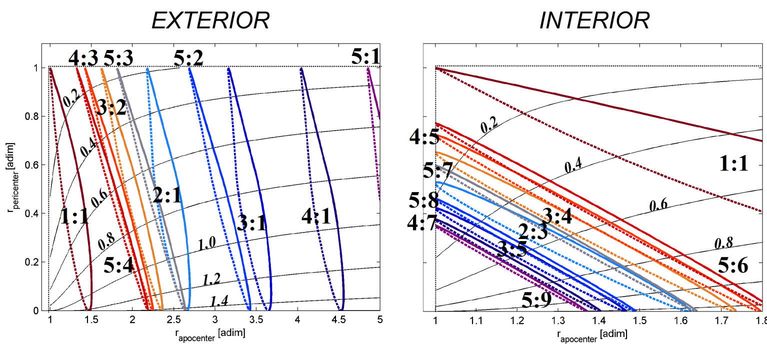

Figure 8 **The *Tisserand Leveraging Graph* in adimensional units obtained plotting the numerical solutions of the VILMs onto the Tisserand graph. We only include the VILMs with $K = m - 1$, as we showed in the previous section they are the most efficient. The solid thick lines are the long transfer VILMs, and the dotted thick lines are the short transfer VILMs.**

- The ΔV_{AB} of the Exterior VILM changes the pericenter but not the apocenter of the spacecraft orbit. We represent the Exterior VILM with a vertical shift from/to the upper boundary of the minor body subdomain.

In Figure 7 we show a schematic Tisserand graph. We use the apocenter-pericenter representation, and show the effect of an Interior and Exterior VILM. We also plot the period level sets and the V_∞ level sets. We clearly see how the ΔV_{AB} changes the V_∞.

We proceed by including the numerical solutions of the VILM. We plot the curves in Figure 4 onto the Tisserand graph, and we obtain the *Tisserand Leveraging Graph*. Figure 8 shows the Tisserand Leveraging Graph in adimensional unit. We only include the VILMs with $K = m - 1$, as we showed in the previous section they are the most efficient. The solid thick lines are the long transfer VILMs, and the dotted thick lines are the short transfer VILMs.

Endgame at Europa using the Tisserand Leveraging graph

In this section we use the Tisserand Leveraging Graph to design Europa endgames starting at $\tilde{V}_{\infty INITIAL} = 1.8$ km/s *. We assume the endgame consists of a series of Forward-Exterior VILMs. We first design one single endgame and then apply the same design strategy in a branch & bound search, storing the total Time

*1.8 km/s is slighty above the $\tilde{V}_\infty$ which can be achieved by multiple gravity assists only.[22,16]

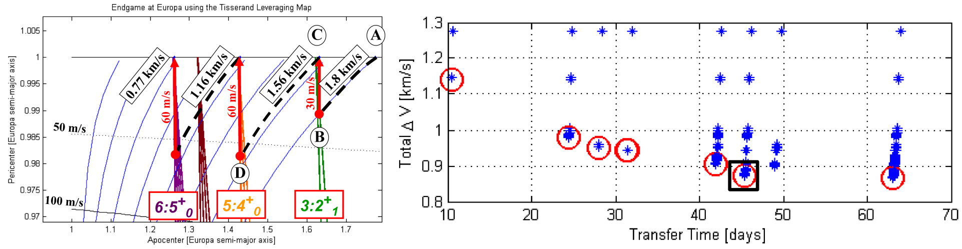

Figure 9 **On the left, simple endgame design using the Tisserand Leveraging Graph. On the right, the result of the *branch&bound* search for the Europa endgame problem with initial velocity of 1.8km/s. The circles are the non-dominated solutions. Among those, the square is the test case presented previously.**

of Flight (ToF) and the total $\Delta\tilde{V}_{TOT} = \sum_i \left(\Delta\tilde{V}_{AB}\right)_i + \Delta\tilde{V}_{\pi EOI}$, where $\Delta V_{\pi EOI}$ is the Europa orbit insertion maneuver:

$$\Delta\tilde{V}_{\pi EOI} = \tilde{V}_{\pi}\left(\tilde{V}_{\infty FINAL}, \tilde{h}_{\pi}\right) - \tilde{V}_c$$

We start designing one Europa endgame, which is a sequence of Forward Interior VILMs. Figure 9 on the left is a close-up of the Tisserand Leveraging Graph scaled to Europa by multiplying the distances by the semi-major axis of the Europa orbit, and by multiplying the velocities by the velocity of Europa. We also plot the level sets of the function $\Delta\tilde{V}_{AB}(\tilde{V}_{\infty L}, \tilde{V}_{\infty H})$ in Eq. (5). The starting point of the endgame is the point A on the figure. The first VILM is composed by a gravity assist and a $\left(\Delta\tilde{V}_{AB}\right)_1$. During the gravity assist, the spacecraft moves along the $\tilde{V}_{\infty} = 1.8$ km/s level set until it intersects , e.g., the $3:2_1^+$ curve (Point B). Then the $\Delta\tilde{V}_{AB}$ at apocenter raises the pericenter to a_M (Point C). Using the $\Delta\tilde{V}_{AB}$ level sets we estimate $\left(\Delta\tilde{V}_{AB}\right)_1 \approx 30m/s$. The transfer time is approx. 3 Europa revolutions (around 10 days) and the new $\tilde{V}_{\infty}$ is around 1.6 km/s. The second VILM consists again of a gravity assist and an impulsive maneuver. The gravity assist moves the spacecraft (r_a, r_p) left and down on the graph until intersecting the $5:4_0^+$ curve (Point D). The second VILM takes some 5 Europa revolutions, it costs some 60 m/s and it reduces the V_{∞} to less than 1.2 km/s. We design the third VILM in the same way and end up with a total transfer time of $6+4+3=13$ Europa revolutions and a total cost of approx $60+60+30=150$m/s, to which we can add the orbit insertion $\Delta\tilde{V}_{\pi}$ for $\tilde{V}_{\infty FINAL} = 0.8$ km/s and the desired $\tilde{h}_{\pi}$.

This recursive strategy is well-suited for a *branch&bound* search, because starting from a fixed $\tilde{V}_{\infty INITIAL}$ the algorithm recursively applies Forward-Exterior VILMs and stores the ToF and total cost of the Endgame. The result of the *branch&bound* search is shown in Figure 9 on the right, where we plot some of the solutions (the stars) and the non-dominated solutions (circle). The test case explained previously is one of the non-dominated solutions (the square). The branch and bound solutions from Figure 9 on the right agree qualitatively with those from[23] that are found using an enumerative method based on dynamic programming principles.

MINIMUM AND MAXIMUMΔV ENDGAME USING VILMS

In this section we use the free-phasing formula introduced previously to discuss the efficiency of the endgame in terms of total ΔV. We first prove that the cost of a sequence of VILMs decreases when favoring high altitude gravity assist. Then we use this result to compute the minimum and maximum cost of a multiple V_{∞} -leveraging transfer, with a focus on the Europa endgame. Future works will include minimum time estimates. Finally we compute the minimum and maximum cost of a multiple V_{∞}- leveraging transfer between different moons, with focus on the Ganymede-Europa transfer.

Efficiency of the V_∞- leveraging

In this section we are interested in the efficiency of the VILMs in terms of ΔV.

Theorem - The total ΔV of a sequence of VILMs decreases when favoring VILMs with high altitude gravity assists.

PROOF: We recall the definition of the phase-free efficiencies of Eq. (6) and Eq. (8):

$$\epsilon_{BI-FE} \equiv \frac{\Delta V_{AB} + \Gamma}{V_{\infty H}} \qquad \epsilon_{BE-FI} \equiv \frac{\Delta V_{AB} + \Gamma}{V_{\infty L} + \Delta V_{AB} \frac{d\Gamma}{dV_{\infty L}}}$$

We recall that $\Gamma > 0$. Thus for $\Delta V_{AB} \longrightarrow 0$, $\epsilon_{BI-FE} > 0$ and $\epsilon_{BE-FI} > 0$. Now compute the variation of the efficiency due to a variation of ΔV_{AB}:

$$\begin{aligned} \frac{\partial \epsilon_{BI-FE}}{\partial \Delta V_{AB}} (\Delta V_{AB}) &= \frac{V_{\infty H} - (\Delta V_{AB} + \Gamma)(D_2 V_{\infty H})}{V_{\infty H}^2} = \\ &= \frac{V_{\infty H}^2 - (\Delta V_{AB} + \Gamma)^2}{V_{\infty H}^3} = -\frac{\Gamma^2 - V_{\infty L}^2}{V_{\infty H}^2} < 0 \end{aligned}$$

$$\frac{\partial \epsilon_{BE-FI}}{\partial \Delta V_{AB}} (\Delta V_{AB}) = -\frac{\Gamma \frac{d\Gamma}{dV_{\infty L}} - V_{\infty L}}{\left(V_{\infty L} + \Delta V_{AB} \frac{d\Gamma}{dV_{\infty L}}\right)^2} < 0$$

where we used $\Gamma > V_{\pi L} > V_{\infty L}$ for the first equation , and $\Gamma \frac{d\Gamma}{dV_{\infty L}} > V_{\infty L}$ (proved in APPENDIX B) for the second equation. Thus both ϵ_{BI-FE} and ϵ_{BE-FI} are positive at $\Delta V_{AB} = 0$ and strictly decreasing with ΔV_{AB}: The efficiencies are at their maximum when $\Delta V_{AB} \longrightarrow 0$, i.e. for small impulsive maneuvers that - when multiple VILMs are patched together - requires high altitude gravity assist. Because this is true for any initial relative velocity, the cost of a sequence of VILMs decreases if we use more VILMs with low-ΔV_{AB} as opposed to fewer VILMs with large ΔV_{AB}. In practice, flight time consideration will limit the number of feasible VILMs.

Q.E.D.

The previous theorem is more intuitive when looking at the level sets of $V_{\infty H}(V_{\infty L}, \Delta V_{AB})$ in Eq. (4), as explained in the following.

Figures 10 show the curves $V_{\infty H}(V_{\infty L}, \Delta V_{AB})$ for the Europa endgame case. At each gravity assist the spacecraft moves along a $V_{\infty H}$ level set. The VILM moves the spacecraft coordinates vertically from top to bottom.

The endgame discussed in the previous section (on the left) is composed of three VILMs for a total transfer time of 46 day and a total ΔV of 154 m/s to reduce the $\tilde{V}_\infty$ from 1.8 km/s to 0.77 km/s. On the right we show a hypothetical endgame composed of fourteen VILMs, each using 10m/s for a total of 140 m/s. The second strategy is cheaper in terms of ΔV (it certainly has a much larger transfer time), because the slope of the curves $\Delta V(V_{\infty L})$ is larger for higher ΔV. Note in fact that

$$\frac{\partial \Delta V_{AB}}{\partial V_{\infty L}} = -\left(\epsilon_{BE-FI}\right)^{-1} \tag{11}$$

Thus the cheapest way to move from an initial to a final V_∞ is by zigzagging "low" on the $x-axis$. This suggest a simple strategy to compute the the minimum ΔV of the VILM transfer, which we explain in the next section. Conversely the more expensive way to move from an initial to a final V_∞ is by performing one unique VILM.

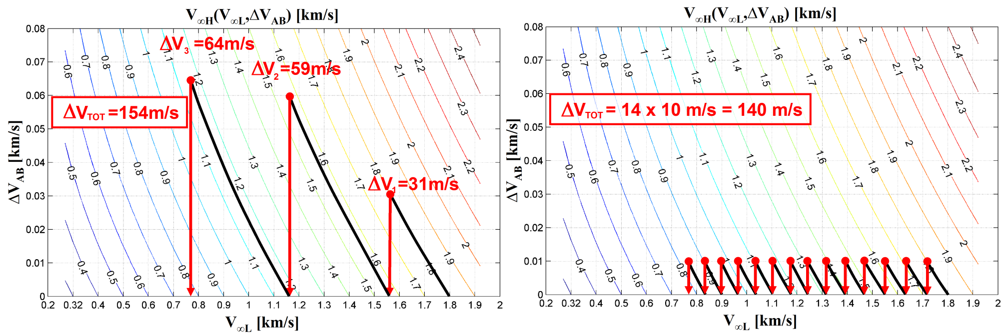

Figure 10 In this figure we compare the endgame at Europa computed in the previous section (on the left), with a hypothetical endgame composed by 14 VILMs (on the right solution). The hypothetical endgame (on the right) is composed of several low-ΔV_{AB}, high altitude gravity assist. The cost of the hypothetical endgame is lower because of the slope of the level sets, which is also related to the phase-free efficiency.

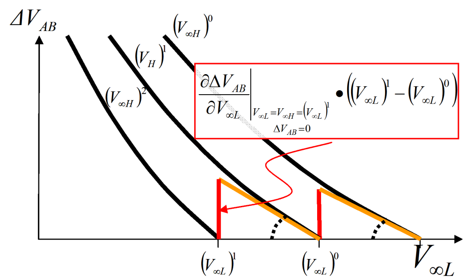

Figure 11 The slope of the $V_{\infty H}$ level sets at $\Delta V_{AB} = 0$ can be used to estimate the ΔV_{AB} for a sequence of VILMs between infinitesimally close V_∞'s .

Theoretical Minimum and Maximum ΔV for VILM transfers with V_∞ boundary conditions

In this section we compute the minimum and maximum ΔV cost to transfer from a $V_{\infty H}$ to $V_{\infty L}$ through a sequence of VILMs. We also compute the minimum and maximum cost for a transfer between two minor bodies $M1$ and $M2$ (with $\tilde{a}_{(M1)} < \tilde{a}_{(M2)}$) , where the boundary conditions are expressed as relative velocity at the first minor body $V_{\infty(M1)}$ and at the second minor body $V_{\infty(M2)}$ (we assume both velocities are larger than the respective $\overline{V}_\infty$).

In the previous section we showed that the minimum ΔV is achieved for infinite transfer times , and infinite altitude gravity assists. We recall that the linked-conics model is less and less accurate for high altitude gravity assist, thus we do not exclude the existence of cheaper transfers computed in more accurate models. The interested reader is referred to.[11,4,13,24] In fact, in our second paper on resonant transfers we explain how the patched three-body problem allows for cheaper (even ballistic) transfers even when the VILM sequence requires a minimum ΔV of several hundred meters per second. However, cheaper transfers are at the expense of larger times of flight - and larger radiation doses for missions to Europa; thus the VILM approach and fast transfers are still used by ESA and NASA to compute the nominal trajectories to Europa and Ganymede. In this context, the theoretical minimum ΔV is a valuable piece of information during the design of resonant transfers as it sets the limit of the VILM approach. Further, as the Pareto front in Figure 9 on the right shows, the variation in ΔV across the full flight time spectrum is generally not more than 10% . The minimum ΔV calculation is the main result of this paper as it provides a simple, fast, and accurate estimate for a preliminary total ΔV cost for any moon tour.

From the previously discussed theorem , and also looking at Figures 10 and 11, it follows that the minimum ΔV needed to transfer from two different V_∞'s is the integral of the slope of the level sets $V_{\infty H}\left(V_{\infty L}, \Delta V_{AB}\right)$ at ΔV= 0.

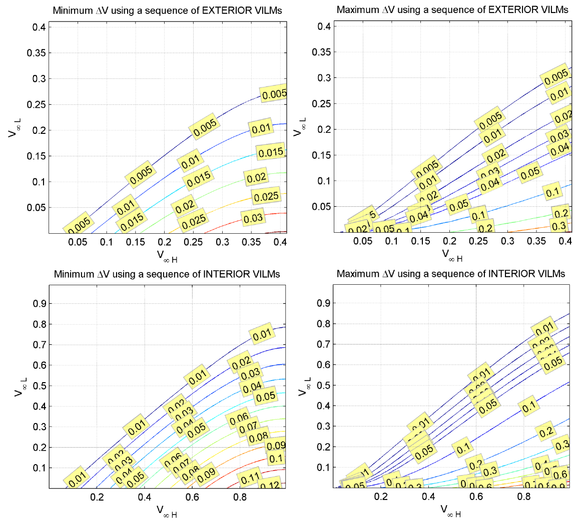

Figure 12 ΔV_{min} **(left) and** ΔV_{max}**(right) of a sequence of Exterior (top) and Interior (bottom) VILMs to change the** V_∞ **from/to** $V_{\infty H}$ **and** $V_{\infty L}$**. The results are in adimensional units. To find the cost for an endgame at Europa, e.g., we multiply all the values by the velocity of Europa.**

From Eq. (11) and Eq. (8) we find:

$$\left.\frac{\partial \Delta V_{AB}}{\partial V_{\infty L}}\right|_{\substack{V_{\infty L}=V_\infty \\ \Delta V_{AB}=0}} = -\frac{V_\infty}{\Gamma(V_\infty)}$$

where we recall that for $V_{\infty L} = V_{\infty H} = V_\infty$ when $\Delta V_{AB} = 0$. Then the minimum cost problem between $V_{\infty L}$ and $V_{\infty H}$ is reduced to simple quadrature:

$$\Delta V_{min}^{(E,I)}\left(V_{\infty L}, V_{\infty H}\right) = \int_{V_{\infty L}}^{V_{\infty H}} \frac{V_\infty}{\Gamma^{(E,I)}(V_\infty)} dV_\infty \tag{12}$$

Using the definition of Γ in Eq. (25), we rewrite Eq. (12) as

$$\Delta V_{min}^{(E,I)}\left(V_{\infty L}, V_{\infty H}\right) = \int_{V_{\infty L}}^{V_{\infty H}} \frac{V_\infty^3 \pm 3V_\infty^2 + V_\infty \mp 1}{V_\infty^3 \pm 3V_\infty^2 - V_\infty \mp 7} dt \tag{13}$$

where the integral can be solved numerically with quadrature or with partial fractions. We recall that $0 \leq V_\infty \leq \sqrt{2} - 1$ for the Exterior VILM, and $0 \leq V_\infty \leq 1$ for the interior VILM.

The maximum ΔV is obtained by performing one unique VILM connecting $V_{\infty H}$ and $V_{\infty L}$, and the formula is given by Eq. (5):

$$\Delta V_{max}\left(V_{\infty L}, V_{\infty H}\right) = -\Gamma + \sqrt{\Gamma^2 + \left(V_{\infty H}^2 - V_{\infty L}^2\right)} \tag{14}$$

Note that $\Delta V_{max} = V_{\infty H}$ if $V_{\infty L} = 0$.

In Figure 12 we show the ΔV_{min} and the $\Delta V_{max}$to increase or reduce the V_∞using a sequence of Exterior or Interior VILMs.

Now we compute the minimum ΔV for transfers between two minor bodies $M1$ and $M2$ (with $\tilde{a}_{(M1)} < \tilde{a}_{(M2)}$). We start by defining $\tilde{V}_{\infty(M1)}^{(h)}$ and $\tilde{V}_{\infty(M2)}^{(h)}$ as the (dimensional) relative velocities at $M1$ and $M2$ of the Hohmann transfer between the two minor bodies. We can use the scale factors associated to $M1$ and $M2$ respectively to compute:

$$V_{\infty(M1)}^{(h)} = \sqrt{\frac{2a_{M2}}{1+a_{M2}}} - 1 \qquad V_{\infty(M2)}^{(h)} = 1 - \sqrt{\frac{2a_{M1}}{a_{M1}+1}} \tag{15}$$

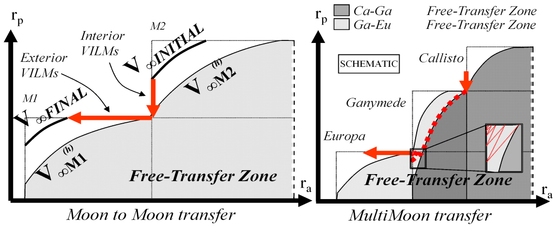

Figure 13. **Minimum VILM Moon-to-Moon transfer (left) and MultiMoon Transfer (right).**

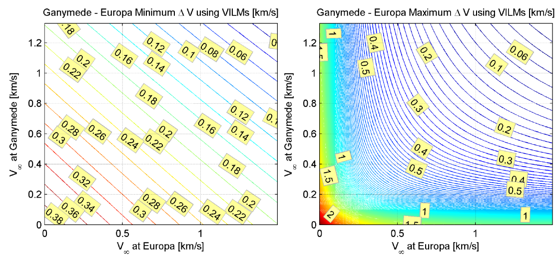

Figure 14. **Minimum and Maximum cost, VILM transfers between Ganymede and Europa with V_∞ boundary conditions.**

The Tisserand's graph in Figure 13 shows that the transfer is free if both $\tilde{V}_{\infty(M1)}$ and $\tilde{V}_{\infty(M2)}$ are greater than $\tilde{V}^{(h)}_{\infty(M1)}$ and $\tilde{V}^{(h)}_{\infty(M2)}$. Figure 13 also suggests that the logical strategy for the minimum ΔV transfer consists of a sequence of Interior VILMs at $M2$, followed by the Hohmann transfer, and finally a sequence of Exterior VILM at $M1$. Then ΔV_{min} is compute applying Eq. (13) twice, first from $V_{\infty H} = V_{\infty INITIAL}$ to $V_{\infty L} = V^{(h)}_{\infty(M2)}$, and then from $V_{\infty H} = V^{(h)}_{\infty(M1)}$ to $V_{\infty L} = V_{\infty FINAL}$. The ΔV_{max} is then computed using Eq. (14) instead of Eq. (13).

Figure 13 on the right shows that other minor bodies can be used to decrease the total $\Delta\tilde{V}$. In the case of a transfer from Callisto to Europa using Ganymede, for example, we only need to increase the initial $\tilde{V}_{\infty(Ca)}$ until $\tilde{V}^{(h)}_{\infty(Ca)}$ to reach the Free-Transfer Zone. Then gravity assists at Ganymede, Europa and Callisto can move the spacecraft to $\tilde{V}^{(h)}_{\infty(Eu)}$, where we start using VILMs at Europa until reaching the desired $\tilde{V}_{\infty(Eu)}$.

Using this notion, together with Eq. (13), Eq. (14), and Eq. (15), we can compute the minimum and maximum $\Delta\tilde{V}$ for any VILM transfer. We apply these formulae for a transfer between Europa and Ganymede, and plot the results in Figure 14.

Theoretical Minimum and Maximum$\Delta\tilde{V}$ for transfers with h_π boundary conditions

In this section we compute the $\Delta\tilde{V}$ for a sequence of VILMs connecting a circular orbit at $M1$ with a circular orbit at $M2$. Pushing the VILM model to its limit, we start considering $r_\pi \rightarrow \infty$. In this case $V_c, \overline{V}_\infty, V_\pi, V_{\infty L} \rightarrow 0$ and the maximum ΔV given by the formula Eq. (14), which also corresponds to the cost of a Hohmann transfer ΔV when no VILM is implemented. In general, we consider the Hohmann transfer as the ΔV_{max} to transfer from given circular orbits.

The minimum cost is computed using Eq. (13). In particular, the cost to reach the $\tilde{V}^{(h)}_{\infty(M1)}$ and $\tilde{V}^{(h)}_{\infty(M2)}$ in the $M1$ and $M2$ adimensional units are :

$$\Delta V_{(Mi)}\left(V_{c(Mi)}\right) = \overline{V}_{\pi(Mi)}\left(V_{c(Mi)}\right) - V_{c(Mi)} + \int_{\overline{V}_{\infty(Mi)}\left(V_{c(Mi)}\right)}^{V^{(h)}_{\infty(Mi)}} \frac{V_\infty}{\Gamma} dV_\infty \quad i = 1, 2 \tag{16}$$

The first two terms on the r.h.s of Eq. (16) represent a propulsive maneuver at periapse of the escape or insertion hyperbola. This maneuver is the escape or capture orbit insertion maneuver$(\Delta V_{escape}, \Delta V_{capture})$

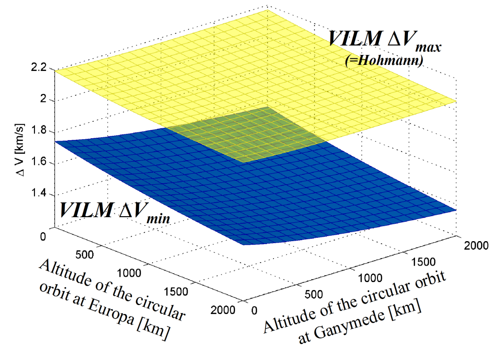

Figure 15. **Minimum VILM transfer between Ganymede and Europa with h_π boundary conditions.**

required to reach the $\overline{V}_\infty$ (the minimum V_∞ where it becomes efficient to start using VILM). The integral term represents the minimum endgame or begingame $(\Delta V_{endgame}, \Delta V_{begingame})$ to reach the Hohmann transfer conditions. Note that the total cost is a function of V_c, i.e. of the altitudes h_π.

The total minimum cost in dimensional units is:

$$\Delta\tilde{V} = \Delta V_{(M1)}\tilde{V}_{M1} + \Delta V_{(M2)}\tilde{V}_{M2}$$

In Figure 15 we show the minimum and maximum $\Delta\tilde{V}$ to transfer from a circular orbit at Ganymede to a circular orbit at Europa (or viceversa). The maximum cost is the $\Delta\tilde{V}$ computed with a direct escape/arrival into the hyperbolic orbits of the Hohmann transfer.

Table 1 and 2 show the minimum and maximum $\Delta\tilde{V}$ [km/s] for transfers between moons in the Jupiter System and in the Saturn System. The minimum $\Delta\tilde{V}$ is the cost of the escape, begingame, endgame, and capture. All the initial and final circular orbits are at 100 km altitude, except for the orbits at Titan, which are at 1500 km altitude.

Table 2 shows the same results for transfers with intermoon gravity assists. In this case the cost of the transfer is significantly reduced because the spacecraft only need to reach the closest moons where it can start performing several gravity assists at different moons, as explained previously and suggested in Figure 13 on the right.

Table 3 shows the semi-major axis and physical data* used in the computation of the minimum $\Delta\tilde{V}$. We also show the radius of the circular orbits, and the corresponding $\tilde{\overline{V}}$ in case of exterior and interior VILMs. The velocity of the moon $\tilde{V}_M$ is the scale factor for all the velocities.

CONCLUSION

In this paper new formula for the V_∞ leveraging maneuver (VILM) are presented. We use these formula to show that the VILM is only efficient when the V_∞ is larger than a minimum value. We also use the formula to build a new graphical tool, the Leveraging Graph, which gives insight on the VILM problem and allows for a fast, intuitive, preliminary design of VILM transfers. The analysis of the VILM efficiency reveals that the total ΔV of a sequence of VILMs decreases when implementing high altitude gravity assists. This suggest a simple way to compute the theoretical minimum ΔV to transfer a spacecraft between arbitrary initial conditions using sequences of VILMs. The minimum ΔV is found by solving a simple quadrature formula. We use this formula to compute the minimum ΔV for different transfers between the Jupiter or Saturn moons. This new design capability is the main result of the paper. The Leveraging Graphs and associated formulae provide for a fast, accurate method for estimating flight time and ΔV trades on the complex endgame and general multi-moon tour problems

*http://ssd.jpl.nasa.gov/

Transfer	ΔV_{min} (km/s)	ΔV_{max} (km/s)	ΔV_{min} (km/s) - *details*			
			ΔV_{escape}	$\Delta V_{begingame}$	$\Delta V_{endgame}$	$\Delta V_{capture}$
Callisto-Ganymede	1.81	2.13	0.73	0.13	0.13	0.81
Callisto-Europa	1.94	3.75	0.73	0.3	0.31	0.59
Callisto-Io	2.43	6.00	0.73	0.46	0.48	0.75
Ganymede-Europa	1.71	2.18	0.82	0.14	0.16	0.59
Ganymede-Io	2.3	4.38	0.82	0.36	0.37	0.75
Europa-Io	1.76	2.54	0.6	0.21	0.2	0.75
Titan-Rhea	1.15	2.19	0.64	0.15	0.18	0.18
Titan-Dione	1.28	3.33	0.64	0.23	0.27	0.14
Titan-Tethys	1.37	4.31	0.64	0.29	0.33	0.11
Titan-Enceladus	1.43	5.27	0.64	0.33	0.4	0.06
Rhea-Dione	0.52	1.12	0.18	0.10	0.10	0.14
Rhea-Tethys	0.66	2.3	0.18	0.19	0.19	0.11
Rhea-Enceladus	0.78	3.53	0.18	0.27	0.27	0.06
Dione-Tethys	0.42	0.97	0.14	0.08	0.09	0.11
Dione-Enceladus	0.55	2.19	0.14	0.17	0.18	0.06
Tethys-Enceladus	0.34	1.00	0.11	0.08	0.09	0.06

Table 1 **Minimum and maximum $\Delta\tilde{V}$ for transfers between moons using VILMs. The transfers start and end at two circular orbits with high or low altitude. The minimum $\Delta\tilde{V}$ is computed assuming infinite transfer time, and consists of a $\Delta\tilde{V}_{escape}$,$\Delta\tilde{V}_{begingame}$,$\Delta\tilde{V}_{endgame}$,$\Delta\tilde{V}_{capture}$. The maximum $\Delta\tilde{V}$ is the cost of the Hohmann transfer without VILMs. Note that using multi-body dynamics it can be possible to find long transfers which require lower $\Delta\tilde{V}$s than the one in this table.**

Transfer	ΔV_{min} (km/s)	ΔV_{max} (km/s)	ΔV_{min} (km/s) - *details*			
			ΔV_{escape}	$\Delta V_{begingame}$	$\Delta V_{endgame}$	$\Delta V_{capture}$
Callisto-G-Europa	1.61	2.07	0.73	0.13	0.16	0.59
Callisto-G-E-Io	1.81	2.35	0.73	0.13	0.2	0.75
Ganymede-E-Io	1.91	2.45	0.82	0.14	0.2	0.75
Titan-R-Dione	1.03	1.55	0.64	0.15	0.099	0.14
Titan-R-D-Tethys	0.98	1.47	0.64	0.15	0.086	0.11
Titan-R-D-T-Enceladus	0.93	1.5	0.64	0.15	0.086	0.061
Rhea-D-Tethys	0.47	1.04	0.18	0.097	0.086	0.11
Rhea-D-T-Enceladus	0.43	1.07	0.18	0.097	0.086	0.061
Dione-T-Enceladus	0.37	1	0.14	0.084	0.086	0.061

Table 2 **Minimum $\Delta\tilde{V}$ for transfers between moons using VILMs and gravity assists. The minimum $\Delta\tilde{V}$ is computed assuming infinite transfer time. The maximum $\Delta\tilde{V}$ is the cost of the Hohmann transfers to the closest inner/outer moons. Using multi-body dynamics it might be possible to find long transfers which require lower $\Delta\tilde{V}$s than the one in this table.**

Moon	$\tilde{\mu}_M\,(km^3/s^2)$	$\tilde{a}_M\,(km)$	$\tilde{V}_M\,(km/s)$	$\tilde{r}_\pi\,(km)$	$\tilde{\tilde{V}}_\infty\,(\tilde{r}_\pi)$ E/I (km/s)
Io	5960	421800	17.330	1922	0.351 / 0.368
Europa	3203	671100	13.739	1661	0.277 / 0.290
Ganymede	9888	1070400	10.879	2731	0.372 / 0.404
Callisto	7179	1882700	8.203	2510	0.328 / 0.361
Enceladus	7	238040	12.624	352	0.029 / 0.029
Tethys	41	294670	11.346	633	0.052 / 0.052
Dione	73	377420	10.025	662	0.067 / 0.068
Rhea	154	527070	8.484	864	0.085 / 0.087
Titan	8978	1221870	5.572	4076	0.283 / 0.321

Table 3. Moon data used for the computation of the minimum ΔV.

ACKNOWLEDGMENT

The authors would like to thank Jon Sims (JPL), Anastassios Petropouls (JPL), Arnaud Boutonnet (ESA), Nathan Strange (JPL) and Shane Ross (VirginiaTech) for their valuable comments.

NOTATION

$\tilde{x}$ Tilde indicates dimensional variable.

P/M Subscript indicates the quantity is referred to the major body (P) or minor body (M).

L Point of the $V_\infty-$leveraging maneuver (VILM) where the spacecraft orbit is tangent to the minor body orbit with a low relative velocity $V_{\infty L}$. Subscript indicates a quantity evaluated at this point.

$H^\pm$ Points of the $V_\infty-$leveraging maneuver where the spacecraft orbit crosses the minor body orbit. There are two possible crossing: H^+ corresponds to the longer transfer and H^- corresponds to the shorter transfer. Subscripts indicate a quantity evaluated at the corresponding point.

A/B Point in the spacecraft trajectory where the impulsive maneuver takes place. The state A belongs to the orbit ending / starting at L, the state B belongs to the orbit ending/starting at H.

ΔV_{AB} Impulsive maneuver at the point A, B.

r_A Distance from the point A, B to the major body.

V_∞ Relative velocity of the spacecraft at the minor body.

V_π Velocity of the spacecraft with respect to the minor body at the pericenter of the hyperbola.

V_c Velocity of the spacecraft at a circular orbit with altitude h_π around a moon with gravitational constant μ_M.

h_π Altitude of the spacecraft closest approach to the minor body.

r_M Radius of the minor body.

a_M Semi-major axis of the minor body (=1 in adimensional units).

V_M Velocity of the minor body with respect to the major body (=1 in adimensional units).

μ Gravitational constant.

$\pm$ In the formula, the plus sign is used for Exterior VILMs and the minus is used for the Interior VILM. If superscript of H, it refers to the short/long transfer.

E/I Superscripts indicates the quantity is referred to an Exterior/Interior VILM.

REFERENCES

[1] J. R. Johannesen and L. A. D'Amario, "Europa Orbiter Mission Trajectory Design," *AAS 99-360*, 1999.

[2] G. Hollenbeck, "New Flight Techniques for Outer Planet Missions," *AAS Paper 75-087 AIAA/AAS Astrodynamics Specialist Conference, Nassau, Bahamas, July 1975*, 1975.

[3] J. A. Sims, J. M. Longuski, and A. Staugler, "V-infinity Leveraging for Interplanetary Missions: Multiple-Revolution Orbit Techniques," *Journal of Guidance, Control and Dynamics*, Vol. 20 n 3, 1997, pp. 409–415.

[4] S. D. Ross and D. J. Scheeres, "Multiple Gravity Assist, Capture and Escape in the Restricted Three-Body Problem," *SIAM Journal on Applied Dynamical Systems*, Vol. 6 n 3, 2007, pp. 576–596.

[5] A. Boutonnet, P. d. Pascale, and E. Canalias, "Desing of the Laplace Mission," *Paper IAC-08-C1.6, 59th IAC, Glasgow, Scottland*, 2008.

[6] J. V. McAdams, D. W. Dunham, R. W. Farquhar, A. H. Taylor, and B. G. Williams, "Trajectory design and maneuver strategy for the MESSENGER mission to mercury," *Journal of spacecraft and rockets*, Vol. 43 5, 2006, pp. 1054–1064.

[7] Y. Langevin, "Chemical and Solar Electric Propulsion option for a Cornerstone Mission to Mercury," *acta astronautica*, 2000.

[8] R. Jehn, S. Campagnola, D. Garcia, and S. Kemble, "Low-Thrust Approach and Gravitational Capture at Mercury," *18th International Symposium on Space Flight Dynamics*, Vol. 548 of *ESA Special Publication*, 2004, p. 487.

[9] T. D. Goodson, D. L. Gray, and Y. Hahn, "Cassini Maneuver Experience: Launch And Early Cruise," *AIAA Paper 98-4224, presented at the AIAA Guidance, Navigation, & Control Conference, Boston, MA, August 10-12,*, 1998.

[10] T. D. Kowalkowski, J. R. Johannesen, and L. Try, "Launch Period Development for the Juno Mission to Jupiter," *AIAA/AAS Astrodynamics Specialist Conference and Exhibiti, Honolulu, Hawaii, August 18 - 21*, 2008.

[11] S. D. Ross and M. W. Lo, "Design of a Multi-Moon Orbiter," *Paper AAS 03-143, AAS/AIAA Space Flight Mechanics Meeting, 9-13 February 2003, Puerto Rico*, 2003.

[12] J. Schoenmaekers, J. Pulido, and J. Cano, "SMART-1 Moon mission: trajectory design using the Moon gravity," tech. rep., ESA, ESOC, SI-ESC-RP-5501, 1999.

[13] P. Grover and S. D. Ross, "Designing Trajectories in a Planet-Moon Environment Using the Controlled Keplerian Map," *Journal of Guidance, Control, and Dynamics*, [accepted].

[14] S. Campagnola and R. P. Russell, "The Endgame Problem Part B: the Multi-Body Technique and the T-P Graph," *Proceedings of the 2009 AIAA/AAS Space Flight Mechanics Meeting*, 2009.

[15] T. H. Sweetser, "Jacobi's Intergal and DeltaV Gravity Assist (DeltaV EGA Trajectories)," *AAS 93-635 AIAA/AAS Astrodynamic Specialist Conference, Victoria, BC, Canada, Aug*, 1993.

[16] M. Vasile and S. Campagnola, "Design of Low-Thrust Multi-Gravity Assist Trajectories to Europa," *Journal of the British Interplanetary Society*, Vol. 62, No. 1, January 2009, pp. 15–31.

[17] R. Abraham, J. E. Marsden, and T. S. Ratiu, *Manifold, Tensor Analysis, and Applications*. Springer, 1988.

[18] A. Labunsky, O. Papkov, and K. Sukhanov, *Multiple Gravity Assist Interplanetary Trajectories*. Earth Space Institute Book Series, Gordon and Breach Publishers, London, 1998.

[19] N. J. Strange and J. M. Longuski, "Graphical Method for Gravity-Assist Trajectory Design," *Journal of Spacecraft and Rockets*, Vol. 39, N. 1, 2002, pp. 9–16.

[20] N. J. Strange and J. A. Sims, "Methods for the design of V-infinity leveraging maneuvers," *AAS/AIAA Astrodynamics Conference, Quebec, Canada, July 30- Aug. 2 2001*, 2001.

[21] A. E. Petropoulos, J. M. Longuski, and E. P. Bonfiglio, "Trajectories to Jupiter via Gravity Assists from Venus, Earth, and Mars," *Journal of Spacecraft and Rockets*, Vol. 37 N.6, 2000, pp. 776–783.

[22] M. Kahn and S. Campagnola, "End-to-End Mission Analysis for a Low-Cost, Two-Spacecraft Mission to Europa," *Proceedings of the 14th AIAA/AAS Space Flight Mechanics Meeting, Maui, Hawaii, February 8-12*, 2004.

[23] A. T. Brinkerhoff and R. P. Russell, "Elliptic Orbits around Planetary Moons," *AAS 09-222 AAS/AIAA Space Flight Mechanics Meeting, Savannah, GA, Feb 2009*, 2009.

[24] E. S. Gawlik, J. E. Marsden, S. Campagnola, and A. Moore, "Invariant Manifolds, Discrete Mechanics, and Trajectory Design for a Mission to Titan," *AAS 09-226, AAS/AIAA Space Flight Mechanics Meeting, Savannah, GA, Feb 2009*, 2009.

APPENDIX A: Derivation of the phase-free formula

From Figure 3 we see that

$$V_L = 1 \pm V_{\infty L} \longrightarrow V_{\infty L}^2 = (V_L - 1)^2 \tag{17}$$

$$V_B = V_A \mp \Delta V_{AB} \longrightarrow V_B^2 = V_A^2 + (\Delta V_{AB})^2 \mp 2V_A \Delta V_{AB} \tag{18}$$

with the upper sign referred to the exterior V_∞leveraging, and the lower sign referred to the interior V_∞leveraging. The velocity of the moon is $V_M^2 = k_P/a_M$. We start considering the leg $L - A$ (the dash lines in Figure 3).

From the vis-viva equation $\frac{1}{2}V_L^2 - 1 = -1/(1 + r_a)$ we obtain:

$$r_A = \frac{V_L^2}{2 - V_L^2} \tag{19}$$

Note that

$$\frac{dr_A}{dV_L} = \frac{4V_L^2}{\left(V_L^2 - 2\right)^2} = \frac{4r_A^2}{V_L^3} \tag{20}$$

and

$$\frac{1}{r_A} = \frac{2}{V_L^2} - 1 \tag{21}$$

From the conservation of the energy and momentum respectively we have:

$$\frac{1}{2}V_L^2 - 1 = \frac{1}{2}V_A^2 - \frac{1}{r_A} \longrightarrow 2\left(1 - \frac{1}{r_A}\right) = V_L^2 - V_A^2 \tag{22}$$

$$V_A = \frac{V_L}{r_A} \tag{23}$$

Using Eq. (21), we have:

$$V_A = \frac{2 - V_L^2}{V_L} \tag{24}$$

We now use r_A in Eq. (19), V_A in Eq. (24), and $V_L$in Eq. (17) to define :

$$\begin{aligned} \Gamma\left(V_{\infty L}\right) &\equiv \pm\left(r_A - V_A\right) = \pm\left(\frac{V_L^2}{2 - V_L^2} - \frac{2 - V_L^2}{V_L}\right) = \\ &= V_{\infty L}\frac{V_{\infty L}^3 \pm 3V_{\infty L}^2 - V_{\infty L} \mp 7}{V_{\infty L}^3 \pm 3V_{\infty L}^2 + V_{\infty L} \mp 1} \end{aligned} \tag{25}$$

Note that Γ is positive, monotonic strictly increasing function of $V_{\infty L}$ because $\Gamma(0) = 0$ and

$$\begin{aligned} \frac{d\Gamma}{dV_{\infty L}} &= \pm\frac{d\Gamma}{dV_L} = \frac{d\left(r_A - V_L/r_A\right)}{dV_L} = \frac{dr_A}{dV_L}\left(1 + V_L/r_A^2\right) - \frac{1}{r_A} = \\ &= \frac{4r_A^2}{V_L^3} + \frac{4}{V_L^2} - \frac{2}{V_L^2} + 1 = \frac{4r_A^2}{V_L^3} + \frac{2}{V_L^2} + 1 > 0 \end{aligned} \tag{26}$$

Now we consider the leg $H - B$.

Considering the triangle composed by V_M, $V_{\infty H}$ and V_H in Figure 2, and using the conservation of momentum:

$$V_{\infty H}^2 = 1 + V_H^2 - 2V_H \cos\gamma = 1 + V_H^2 - 2V_B r_A \tag{27}$$

From the conservation of the energy and from Eq. (22):

$$V_H^2 - V_B^2 = 2\left(1 - \frac{1}{r_A}\right) = V_L^2 - V_A^2 \longrightarrow V_H^2 = V_L^2 + V_B^2 - V_A^2 \tag{28}$$

From combining Eq. (27) and Eq. (28) we get:

$$\begin{aligned} V_{\infty H}^2 &= 1 + V_B^2 - V_A^2 + V_L^2 - 2V_B r_A = \\ &= 1 + (\Delta V_{AB})^2 \mp 2V_A \Delta V_{AB} + V_L^2 - 2V_A r_A \pm 2\Delta V_{AB} r_A = \\ &= 1 + V_L^2 - 2V_L + (\Delta V_{AB})^2 \pm 2\Delta V_{AB}(r_A - V_A) = \\ &= V_{\infty L}^2 + (\Delta V_{AB})^2 \pm 2\Delta V_{AB}(r_A - V_A) \end{aligned} \tag{29}$$

Using the function Γ defined in Eq. (25) we finally get

$$V_{\infty H}^2 = V_{\infty L}^2 + \Delta V_{AB}^2 + 2\Delta V_{AB}\Gamma$$

and also

$$\Delta V_{AB} = -\Gamma + \sqrt{\Gamma^2 + (V_{\infty H}^2 - V_{\infty L}^2)}$$

Note that we exclude the negative root as ΔV_{AB} has to be positive.

APPENDIX B: ON THE SIGN OF $\Gamma \frac{D\Gamma}{DV_{\infty L}} - V_{\infty L}$

First note that:

$$\frac{d\Gamma}{dV_{\infty L}}\Gamma - V_{\infty L} = \frac{1}{2}\frac{d\left(\Gamma^2\right)}{dV_{\infty L}} - V_{\infty L} \tag{30}$$

We recall that:

$$r_A = \frac{V_L^2}{2 - V_L^2} = -\frac{2}{V_L^2 - 2} - 1 \tag{31}$$

$$V_A = \frac{V_L}{r_A} = \frac{2}{V_L} - V_L \tag{32}$$

So that

$$V_A^2 = V_L^2 + \frac{4}{V_L^2} - 4 = V_L^2 + 2\left(\frac{2}{V_L^2} - 1\right) - 2 = V_L^2 - 2\left(\frac{1}{r_A} - 1\right)$$

Also because $\frac{d}{dV_{\infty L}} = \pm\frac{d}{dV_L}$:

$$\frac{dr_A}{dV_{\infty L}} = \pm\frac{dr_A}{dV_L} = \pm\frac{2V_L}{(V_L^2 - 2)^2} \tag{33}$$

Now let's compute:

$$\begin{aligned} \left(\Gamma^2\right) &= (r_A - V_A)^2 = r_A^2 + V_A^2 - 2r_A V_A = r_A^2 + V_L^2 - 2\left(\frac{1}{r_A} - 1\right) - 2V_L \\ &= r_A^2 + \frac{2}{r_A} + (V_L - 1)^2 - 3 = r_A^2 + \frac{2}{r_A} + (V_{\infty L})^2 - 3 \end{aligned}$$

Then

$$\begin{aligned} \frac{d\Gamma}{dV_{\infty L}}\Gamma - V_{\infty L} &= \frac{1}{2}\frac{d\left(\Gamma^2\right)}{dV_{\infty L}} - V_{\infty L} = \frac{1}{2}\left(2r_A - \frac{2}{r_A^2}\right)\frac{dr_A}{dV_{\infty L}} + V_{\infty L} - V_{\infty L} = \\ &= \pm\frac{2V_L}{(V_L^2 - 2)^2}\left(\frac{r_A^3 - 1}{r_A^2}\right) = \pm\left(r_A^3 - 1\right)\frac{2V_L}{(V_L^2 - 2)^2}\frac{(V_L^2 - 2)^2}{V_L^4} = \left|r_A^3 - 1\right|\frac{2}{V_L^3} > 0 \end{aligned}$$